

EVALUATION OF HOT FORMABILITY OF AN AL-4.6ZN-0.8MG ALLOY BY INCREASING-STRAIN-RATE TORSION TESTS

M.El Mehtedi, N. Ryum, S. Spigarelli, E. Evangelista and B. Ronning

***INFM/Dipartimento di Meccanica, Università Politecnica delle Marche, I-60131 Ancona, Italy**

****Department of Materials Technology and Electrochemistry, NTNU, N-7491 Trondheim, Norway**

Abstract

The hot formability of an experimental Al-4.6%Zn-0.8%Mg alloy was studied by torsion testing. Conventional constant strain-rate tests were carried out to investigate material response in selected condition of temperature, T , and strain rate, $\dot{\epsilon}$. In order to determine the relationship relating flow stress with strain rate and temperature, the conventional procedure, based on straining at constant strain rate, requires a relatively large number of tests. The scope for reducing the number of tests by increasing linearly $\dot{\epsilon}$, i.e., where K is a constant, from 0 to a definite value, was explored in this work and a series of increasing strain-rate tests were carried out. Nine tests, with K ranging from 0.05 to 0.2 s^{-1} , were performed at 500 °C; the resulting curves were used to recalculate the iso-strain rate curve; comparison between experimental and calculated curve gave encouraging results, confirming the reliability of both testing procedures. The microstructure of torsioned samples was investigated by light (LM) and scanning electron microscopy (SEM). EBSD patterns were obtained to analyse grain size distribution and the presence of substructures. The results are discussed in the light of the more recent theories of high-temperature deformation of Al alloys.

Riassunto

La lavorabilità a caldo a 500°C di una lega Al-6.2%Zn-0.8%Mg è stata studiata utilizzando prove di torsione condotte secondo una nuova procedura (ISR) che prevedeva una variazione lineare della velocità di angolare ω secondo la legge $\omega = K\theta$ in cui θ era l'angolo di rotazione. In particolare sono state condotte prove con valori di K variabili fra 0.05 e 2 s^{-1} . A titolo di confronto sono state quindi condotte prove di torsione con velocità di deformazione costante (CSR). Le curve tensione equivalente - deformazione equivalente per le prove ISR erano caratterizzate da un aumento monotono della tensione con la deformazione, senza che si arrivasse ad un regime di saturazione. Le curve ottenute con velocità di deformazione costante a 500 °C erano caratterizzate invece da un aumento della tensione fino ad un valore di picco seguito da una modesta diminuzione della tensione di flusso che raggiungeva successivamente il valore stazionario, comportamento tipico dei materiali che non esibiscono ricristallizzazione dinamica. Comunque questa semplice analisi qualitativa della forma delle curve tensione-deformazione non poteva essere considerata una prova conclusiva per escludere l'instaurarsi della ricristallizzazione dinamica.

La microstruttura dei campioni deformati è stata analizzata tramite le usuali tecniche di microscopia ottica ed elettronica in scansione/EBSD. Tali studi hanno dimostrato che con l'aumentare della deformazione al progressivo allungamento dei grani, inizialmente equiassica, si accompagnava la formazione di sottostrutture che erano, per una data deformazione, più fini nelle prove CSR che nelle ISR. Questo risultato si doveva attribuire al fatto che, anche se il valore istantaneo della velocità di deformazione alla fine della prova ISR poteva assumere lo stesso valore di quella CSR, per il resto della prova il materiale veniva deformato a velocità più basse; e' ben noto, infatti, che la dimensione dei sottogranì prodotti dal riarrangiamento delle sottostrutture che si verifica nel corso della deformazione a caldo diventa via via più fine al crescere della velocità di deformazione imposta.

Da quanto esposto emergeva l'esigenza di sviluppare una metodologia di confronto fra i dati ottenuti in condizione di velocità di deformazione costante (cioè nella maggior parte degli studi di laboratorio) e quelli ricavati in condizione di velocità di deformazione variabile come quelli prodotti nel presente studio. Un primo approccio preliminare consisteva nel riportare le curve tensione equivalente - deformazione equivalente di tipo ISR su un grafico bilogarithmico; si osservava quindi che dopo uno stadio iniziale (transiente), i punti relativi alle prove condotte con K diversi si sovrapponevano sulla stessa retta che descriveva la variazione della tensione di picco in funzione della velocità di deformazione ottenute da prove CSR. Si può quindi concludere che dopo lo stadio iniziale, i valori della tensione misurata ad una determinata deformazione (e quindi, a seconda del valore di K , ad una certa velocità di deformazione istantanea) in condizioni ISR siano sostanzialmente equivalenti alla tensione di picco ottenuta in una prova CSR condotta ad una velocità di deformazione uguale a quella istantanea. Questi risultati preliminari, pur suggerendo l'opportunità di condurre a fianco delle convenzionali prove CSR almeno alcune prove ISR, hanno comunque evidenziato la necessità di approfondire alcuni aspetti dell'applicazione di questa nuova metodologia di prova.

INTRODUCTION

The hot formability of Al-Zn-Mg alloys [1-4] and their ageing response [5] have extensively been investigated in the last two decades, by using tension, compression and torsion testing under constant strain rate to obtain equivalent stress vs equivalent strain curves. Traditional tension tests are of limited practical use to investigate hot formability, since instability phenomena, i.e. necking, preclude attainment of the deformation levels usually encountered in hot forming operations, and early fracture occurs well before the steady state or even peak stress is reached. Compression tests are valuable even though, also in this case, deformation is not homogeneous due to barrelling. By contrast, torsion testing is not affected by instability effects and can thus be used to deform materials up to very large equivalent strains (50 or more, in case of pure Al). Analysis of the shape of the flow curves obtained in compression or in torsion and electron microscopic microstructural studies directed the

attention of researchers to defining the exact microstructural phenomena controlling high-temperature deformation in Al alloys. Dynamic recrystallisation (DRX) is generally promoted by a low level of dynamic recovery (DRV), usually an effect of low stacking-fault energy (SFE) and/or of high grain-boundary mobility. Most of aluminium alloys do not dynamically recrystallise due to the high SFE value of this metal [6,7]; yet, in particular cases, as in Al-10%Zn [8] or Al-5Mg-0.7Mn [9], dynamic recrystallisation can be induced by a decrease in SFE due to alloying elements or to the presence of particles. The presence of Mn (and the resulting formation of (Fe,Mn)Al₆ particles) can favour DRX in Al-alloys [10-11]; this observation has been explained with a retarding or accelerating effect on DRX by dispersoids and particles, depending on particle size and spacing [7,10]. As mentioned above, the conventional testing technique consists in deforming samples under constant strain rate; even though this procedure is essential for the proper determination of the constitutive equations relating flow stress with temperature and strain rate, it may entail severe drawbacks, since it does not faithfully represent the usual forming operations, where strain rate increases from 0 to a maximum value. The idea of testing materials under changing strain-rates was conceived in this context. The aim of the present study was thus to test a different experimental technique based on deformation in torsion of an Al alloy with strain rate rising linearly with strain.

EXPERIMENTAL DETAILS

The alloy investigated in the present study had the following chemical composition (wt%): Zn=4.56, Mg=0.81, Fe=0.071, Si=0.028, Ti=0.014, Al=bal. The material was cast in a pilot plant at Roufoss Technology AS (Norway). Aluminum ingots of commercial purity were melted in an induction furnace and pure Mg and Zn added to the melt at 750°C. Non-metallic inclusions and dissolved elements like Hydrogen, Calcium and Sodium were removed from the melt by an Argon flux. Grain refinement was achieved by feeding a master alloy containing 5wt% Ti and 1wt% B into the launder. Billets 15 cm in length were cut from the ingot and subjected to a homogenisation heat treatment consisting in 6 h permanence at 500°C (heating time 3 h).

Torsion tests were carried out at 500°C on two computer-controlled torsion machines. Temperature was controlled by a thermocouple inserted in close proximity of the gauge length. Samples were heated by an induction coil.

Two different types of torsion tests were performed: i) conventional constant strain-rate (CSR) tests (constant angular velocity ω), carried out in two independent laboratories (Trondheim and Ancona); ii) increasing strain-rate (ISR) tests,

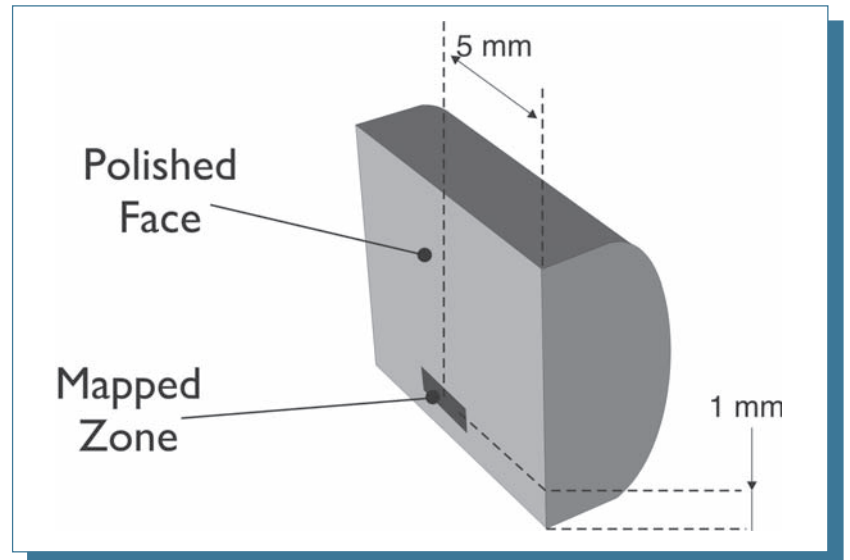


Fig. 1: Schematic representation of the sectioning of the gauge length and of the location of the mapping zone for EBSD

where the angular velocity increased linearly with the angle of twist θ , i.e. $\omega = K\theta$, carried out in Trondheim.

Torque M and the angle θ were used to estimate the equivalent stress on the surface of the samples subjected to ISR tests by using Nadai's formula [12]

$$\sigma = \frac{\sqrt{3}}{2\pi R^3} \left(3M + \frac{\theta \delta M}{\delta \theta} \right) \quad (1)$$

where R is sample radius.

In CSR tests, the equivalent stress on the sample's surface was estimated by the relationship

$$\sigma = \frac{\sqrt{3}M}{2\pi R^3} (3 + p + q) \quad (2)$$

where $P = \frac{\delta \ln M}{\delta \ln \dot{\theta}}$ and $q = \frac{\delta \ln M}{\delta \ln \omega}$ [13]. Since in steady state $p=0$, parameter p was considered 0 also for the rest of the curve; for the sake of simplicity, parameter q was also taken $=0$.

The microstructure of both undeformed and torsioned samples was investigated by light microscopy (LM) and SEM/EBSD; in particular, EBSD maps were obtained by analysing the portion of the sample as illustrated in Fig. 1. Specimens were mechanically ground and polished in 78 ml perchloric acid, 120 ml distilled water and 800 ml ethanol for 3 min at 19V.

RESULTS AND DISCUSSION

The microstructure of the undeformed material at LM and EBSD is shown in Fig.2. The homogenising heat treatment produced large equiaxed grains.

The equivalent-stress vs equivalent-strain curves obtained with CSR tests performed at different revolution rates are plotted in Fig.3; as usual, the flow stress increases with strain rate. At a constant strain rate, flow stress increases with strain up to peak and then decreases to a saturation value (steady state); under this respect, the behaviour of the investigated alloy is similar to that of other Al-alloys where dynamic recrystallisation does not occur. The peculiar oscillatory shape of the curve obtained at 10^{-1} s^{-1} is an interesting aspect requiring investigation since it has previously observed in another series of torsion tests of a similar alloy in a different laboratory [14]. In any case, qualitative analysis cannot provide conclusive indications on the occurrence of DRX.

Figure 4 plots the equivalent stress vs equivalent strain in ISR tests, for K ranging from 0.05 up to 2 s^{-1} . The flow stress increases steadily with strain as strain rate increases, although it obviously does not reach saturation in this condition.

Figure 5 plots a comparison between equivalent-stress vs equivalent-strain curves obtained with CSR ($\omega = 0.9 \text{ rad/s}$) and ISR tests (revolution rate increasing from 0 to 0.9 rad/s) at different k values ($2, 0.2, 0.1, 0.05 \text{ s}^{-1}$); at a given strain, the equivalent stress is higher in the former condition, even though the difference progressively diminishes as the instantaneous strain rate in ISR tests approaches the value of CSR tests.

The microstructure of the deformed alloy along the longitudinal direction of the gauge length 1 mm from the surface is shown in Fig.6. The grain elongation resulting from torsion straining is well documented. Representative examples of the EBSD maps obtained by analysing samples deformed up to 4.5 ($\epsilon=1.3$), 6 ($\epsilon=1.7$) and 9 rad

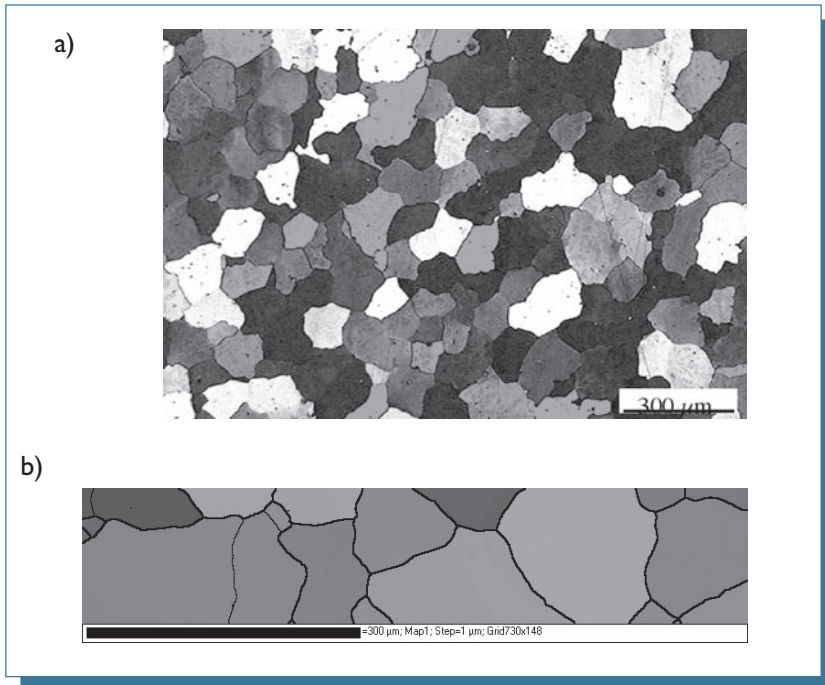


Fig. 2: Microstructure of the undeformed alloy: a) LM; b) EBSD pattern with grains substructure-free (grain size $\approx 155 \mu\text{m}$)

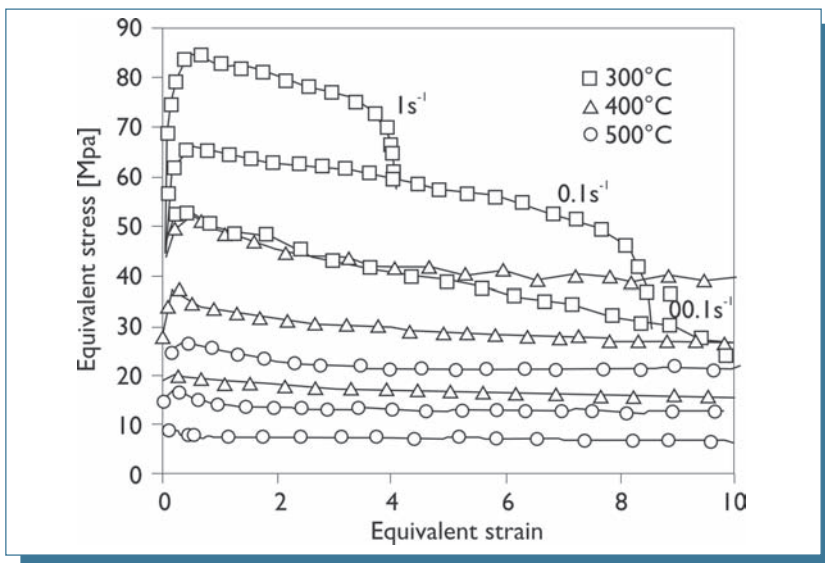


Fig. 3: equivalent-stress vs equivalent-strain curves obtained from CSR tests; strain rate, at a given temperature, decreases from 1 to 10^{-2} s^{-1} from the upper part to the lower one of the figure

($\epsilon=2.6$) are shown in Figs.7-9. The reduction in the transversal section of the grains as the strain increases (corresponding to an elongation in tangential direction, i.e. to the usual increase in aspect ratio typical of non-recrystallised materials tested in torsion) and the parallel formation of substructures (subgrain boundaries) are clearly shown. The reduction in grain section was found to be greater in CSR samples (Fig.10). Subgrain size also appeared to be substantially finer in CSR samples; this was largely expected, since the scale of the substructure (in this case subgrain size) is known to become finer as the strain rate increases [4]. Since for a given strain CSR samples always experience a higher strain rate than the ISR ones (compare with Fig.5), a greater subgrain size would be expected in the latter. The occurrence of dynamic recrystallisation cannot be proved conclusively even though several grains appear to be substructure-free.

Analysis of the above results poses an intriguing question about the procedure that should be followed to compare experimental data obtained with the usual CSR tests and those of ISR tests. Figure 11 presents an attempt at comparing these results. In principle, ISR tests cannot be used to calculate constitutive equations, i.e. the relationships that binding strain rate and temperature with peak of steady state flow stress; yet, Fig.11 plots the flow stress obtained with ISR tests as a function of instantaneous strain rate on double logarithmic coordinates, and the straight line that describes the variation of peak flow stress as a function of strain rate in CSR tests (imposed strain rate ranged from 10^{-3} s^{-1} to 1 s^{-1}). It can easily be observed that, after an initial (transient) stage, the ISR curves largely overlap on the same line of slope close to 5.5, representing the conventional power law

$$\dot{\epsilon} = A \sigma^n \quad (3)$$

being A a temperature-dependent parameter, that, for the alloy in question, can be used to describe the peak flow stress variation with testing strain rate in conventional CSR conditions ($A=10^{-8} \text{ s}^{-1} \text{ MPa}^{-n}$). This behaviour implies that, after an initial transition region, the flow stress at a given strain in ISR tests assumes a value equivalent to the peak flow stress in CSR tests carried out under the strain rate corresponding to the instantaneous strain rate at that strain. Figure 12 shows a comparison between the experimental data

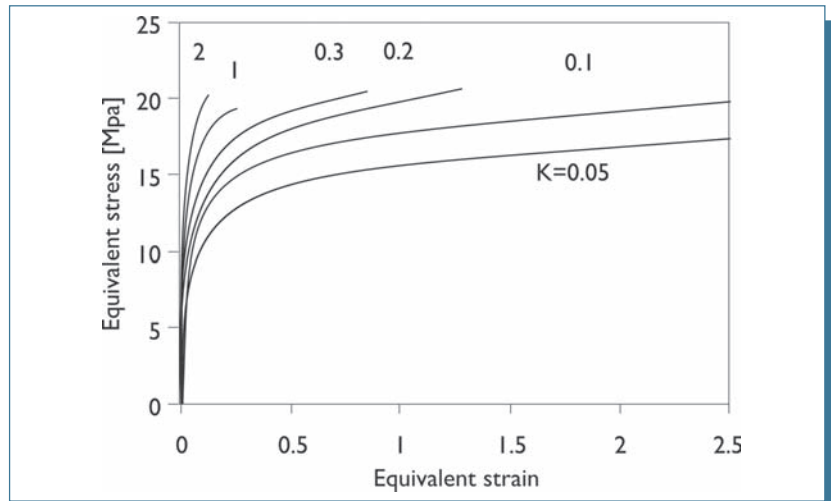


Fig. 4: Equivalent-stress vs equivalent-strain curves obtained from ISR tests (K ranging from 0.05 to 2 s^{-1})

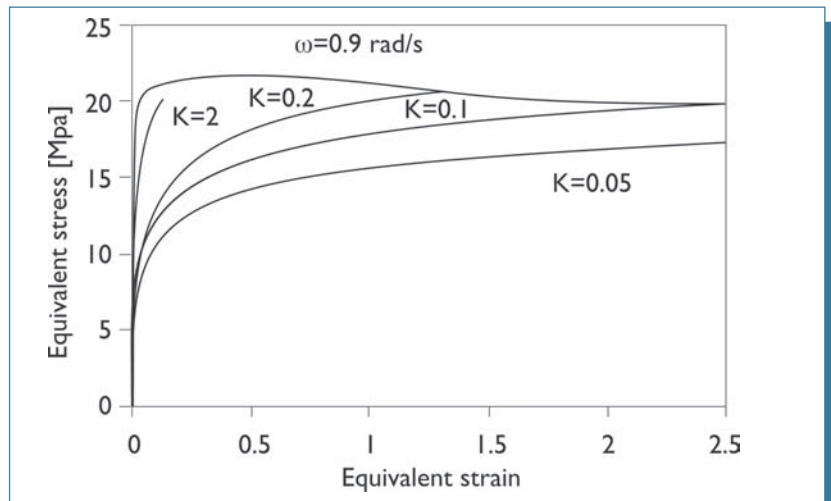


Fig. 5: Comparison between CSR and ISR curves (at different k values)

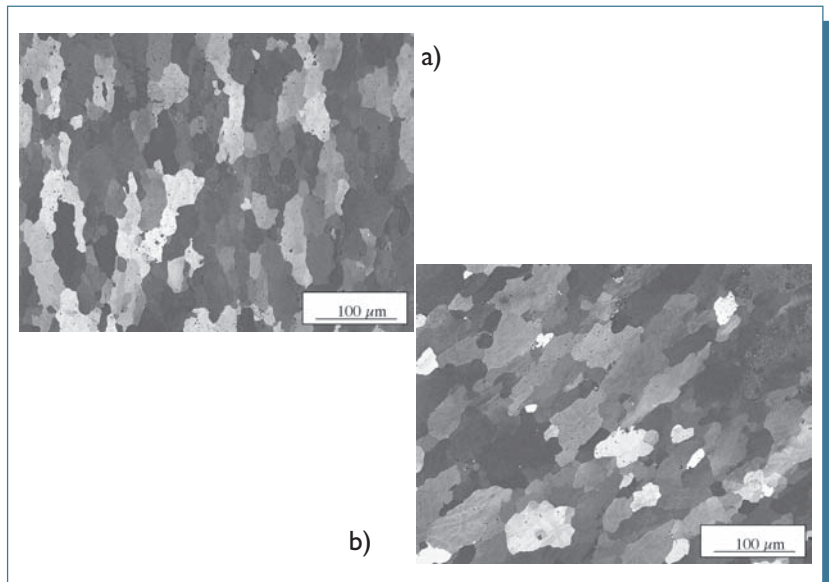


Fig. 6: Microstructure of deformed samples after a torsional strain of 6 rad ($\epsilon=1.7$)
a) CSR test ($\omega=0.6 \text{ rad/s}$); b) ISR test ($K=0.1 \text{ s}^{-1}$)

obtained for $K=0.2$ and the curve calculated by substituting the calculated strain rate ($=K\dot{\epsilon}$) in the power law of Fig. 10; the calculated and the experimental curves agree, providing a first confirmation that ISR and CSR testing procedures give consistent descriptions of the high-temperature response of this alloy. ISR tests simulate more closely the usual hot-forming operations where strain rate, for a given element of material, is expected to increase from 0 to a maximum value and to decrease again subsequently to 0. It follows that an extensive study of the hot workability of a metal should include an optimised mix of both CSR and ISR tests to cover all the fundamentals of mechanical and

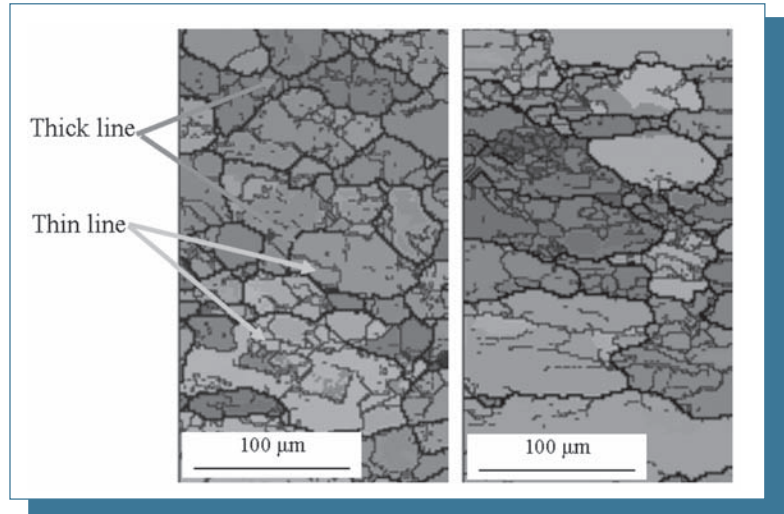


Fig. 7: EBSD pattern of samples deformed after a torsional strain of 6 rad, the thick lines are the high angle boundaries (misorientation angle $\theta > 12^\circ$) and the thin lines are the low angle boundaries ($2^\circ < \theta < 10^\circ$); a) CSR test at $\omega = 0.9$ rad/s (grain size $d_g = 44$ μm ; subgrain size $d_{sg} = 16.2$ μm); b) ISR test with $K = 0.2$ s^{-1} ($d_g = 57$ μm , $d_{sg} = 17.7$ μm)

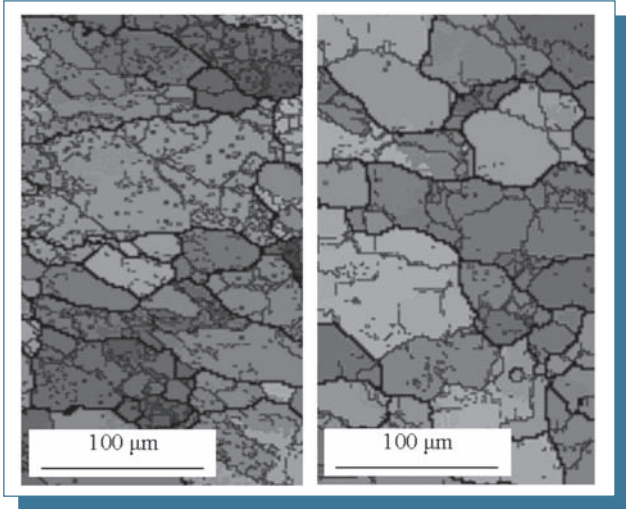


Fig. 8: EBSD maps of samples deformed after a torsional strain of 6 rad; a) CSR test at $\omega = 0.6$ rad/s ($d_g = 48.6$ μm ; $d_{sg} = 16.5$ μm); b) ISR test with $K = 0.1$ s^{-1} ($d_g = 55$ μm , $d_{sg} = 18.7$ μm)

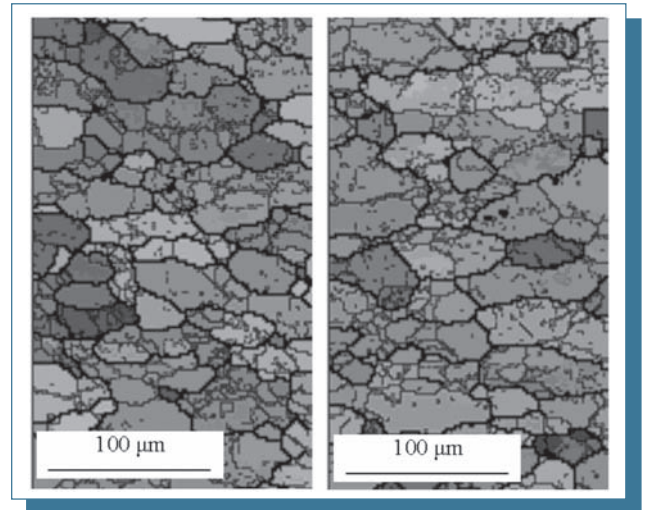


Fig. 9: EBSD maps of samples deformed after a torsional strain of 9 rad; a) CSR test at $\omega = 0.9$ rad/s (grain size $d_g = 41$ μm ; $d_{sg} = 16$ μm); b) ISR test with $K = 0.1$ s^{-1} ($d_g = 46.6$ μm , $d_{sg} = 17.5$ μm)

microstructural response, unless a reliable model converting CSR data to ISR (or vice versa) is available. A further study will thus be devoted [15] to investigation of these aspects.

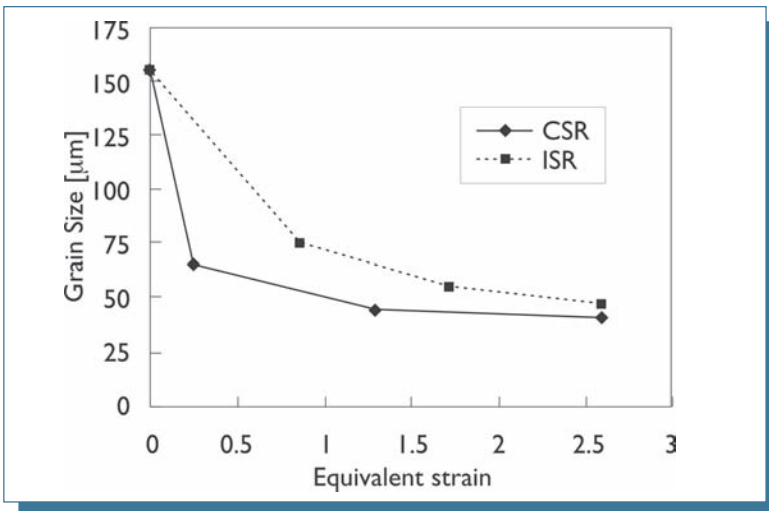


Fig. 10: Grain size measured on EBSD maps

CONCLUSIONS

The hot formability of an experimental Al-4.6%Zn-0.8%Mg alloy was studied by means of torsion testing. Conventional constant (CSR) and increasing (ISR) strain-rate tests were carried out to investigate the material response at 500 °C. Strain rate $\dot{\epsilon}$ changed linearly with strain, i.e. $\dot{\epsilon} = K\epsilon$, where K is a constant, from 0 to a definite value in ISR tests. Nine tests, with K ranging from 0.05 to 0.2, were performed; the resulting curves were used to recalculate the iso-strain rate curve; comparison between experimental and calculated curve gave encouraging results, confirming the reliability of both testing procedures.

The microstructure of torsioned samples was investigated by light (LM) and scanning electron microscopy (SEM). EBSD patterns were obtained to analyse grain size distribution and the presence of substructures.

REFERENCES

- 1] E.Evangelista, E.Bonetti, E.Di Russo, P.Fiorini and H.J.McQueen, Hot working behaviour of high strength 7012 Alumunim Alloy, in *Aluminum Technology 86*, The Institute of Metals, London, 1986, 185-196.
- 2] E.Evangelista, E.Di Russo, H.J.McQueen and P.Mengucci, Mechanical Improvement in 7XXX alloys by different alloying balance, in *Homogenization and Annealing of Al and Cu Alloys*, E.H.Chia and H.D.Merchant Eds., *ASM International*, Metal Park, Ohio, 1988, p.p.209.
- 3] B.Rønning and N.Ryum, *Physical Metallurgy and Materials Science (A)*, volume 32A (2001), 769-776.
- 4] E.Cerri, E.Evangelista, A.Forcellese, H.J.McQueen, *Materials Sci.EngineeringA* 197, (1995) p.p.707.
- 5] G.Thomas and J.Nutting, *Journal of the Institute of Metals*, 88 (1960) 81-90.
- 6] H.J.McQueen and N.Ryum, *Scandinavian Journal of Metallurgy*, 14 (1985) 183-194.
- 7] H.J.McQueen and K.Conrod, Recovery and Recrystallization in the Hot Working of Aluminum Alloys, *Proc. AIME Symp. On Microstructural Control during Al Alloys Processing*, H.Chia and H.J.McQueen Eds., Met.Soc.AIME, Warrendale, Pa, 1985, pp 1-18.
- 8] K.J.Gardner and R.Grimes, *Met.Sci.* 13 (1979) 216-222.
- 9] T.Sheppard and M.G.Tutcher, *Met.Sci.* 14 (1980) 579-589.
- 10] E.Evangelista, H.J.McQueen and E.Bonetti, Interaction between (MnFe)Al₆ particles and substructure formed during hot working of Al-5Mg-0.8Mn alloy, *Proc. 4th International Symp. On Deformation of Multiphase and Particle Containing Materials*, Risø National laboratory, Roskilde, Denmark, 1983, pp. 243-250.
- 11] H.J.McQueen, E.Evangelista, J.Bowles and G.Crawford, *Met.Sci.* 18 (1984) 395-402.
- 12] A.Nadai: *Theory of flow and fracture of solids*, McGraw-Hill Book Company, USA, 1950.
- 13] D.S.Fields and W.A.Backofen: *Proc.Am. Soc. Test. Mater.*, Vol. 57 (1957), 1259-1272.
- 14] B.Rønning: *Ph.D.Thesis*, Norwegian University of Science and Technology, Trondheim, 1998.
- 15] M.El Mehtedi, S.Spigarelli, M.Cabibbo, E.Evangelista, N.Ryum, to be published.

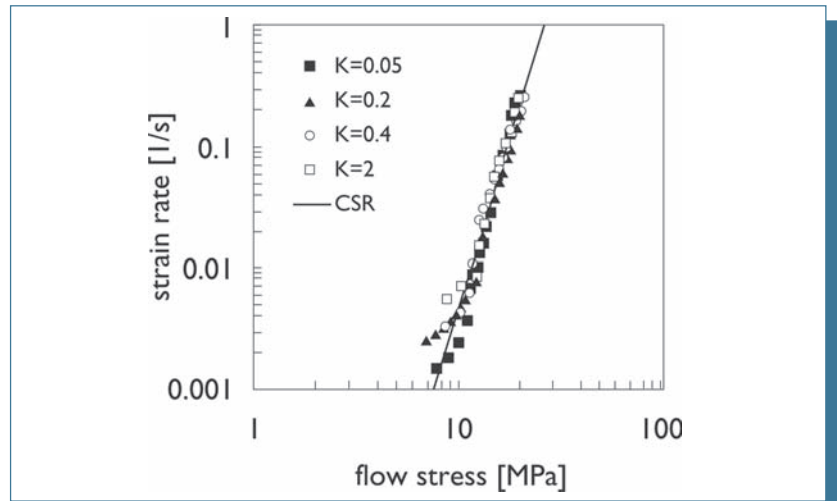


Fig. 11: Comparison between strain rate vs flow stress for representative ISR tests and power law describing the peak flow-stress dependence on strain rate for CSR tests

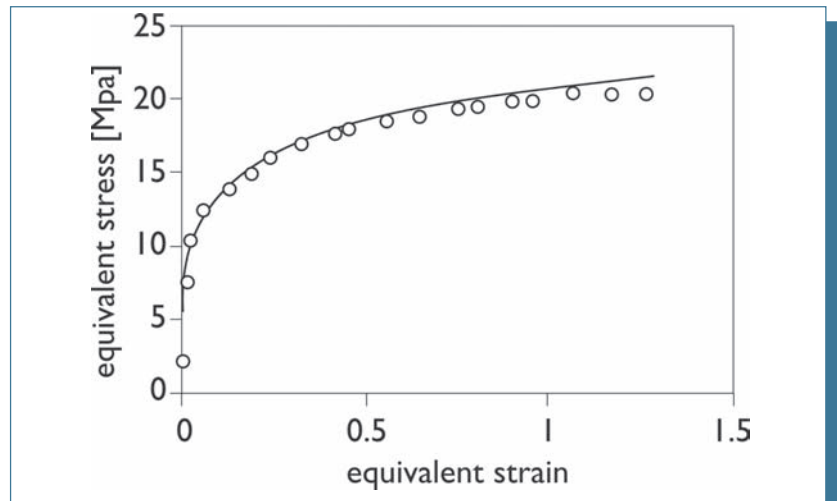


Fig. 12: Comparison between the experimental curve for $K=0.2 \text{ s}^{-1}$ (symbols) and the curve obtained by substituting the nominal strain rate $K\epsilon$ in the power-law equation of Fig. 11